Eradication of neuroblastoma by T cells redirected with an optimized GD2-specific chimeric antigen receptor and interleukin-15

Yuhui Chen[1], Chuang Sun[1], Elisa Landoni[1], Leonid Metelitsa[2], Gianpietro Dotti[1,3], Barbara Savoldo[1,4]

[1]Lineberger Comprehensive Cancer Center, University of North Carolina at Chapel Hill

[2]Department of Pediatrics, Texas Children's Hospital, Houston, TX

[3]Department of Microbiology and Immunology, University of North Carolina at Chapel Hill

[4] Department of Pediatrics, University of North Carolina at Chapel Hill

Corresponding Author: Barbara Savoldo

Address: 125 Mason Farm Road, Marsico Hall 5203, Chapel Hill, NC 27599-7290

Phone: 919-962-8414

Email: bsavoldo@med.unc.edu

Abstract: 238 words

Text: 4648 words

Running title: GD2.CAR-Ts expressing IL-15 eradicate neuroblastoma

Conflict of Interest Statement: The authors have declared that no conflict of interest exists.

1

TRANSLATIONLA RELEVANCE

Responses rates in neuroblastoma (NB) patients receiving GD2.CAR-Ts remain significantly inferior to those observed in patients with acute lymphoblastic leukemia treated with CD19.CAR-Ts. This is consequent to the limited GD2.CAR-Ts survival in the circulation and at the tumor site. To solve these issues, we have incorporated IL-15 within the CAR construct to generate GD2.CAR.15-Ts. These cells enriched in central memory/stem-cell-like cells and expressing PD-1 at lower level promoted superior antitumor activity, expansion and survival *in vitro* and *in vivo*. To improve the safety of the GD2.CAR.15-Ts, we have incorporated the iC9 safety switch gene and validated the feasibility of generating T cell products incorporating the three genes in accordance with good manufacturing practice (GMP). Our discoveries guide an efficient and safe therapeutic option of GD2.CAR-Ts in patients with NB, and are highly relevant for the development of CAR-T for solid tumors in general.

2

ABSTRACT

Purpose: A delay in encountering the cognate antigen while in the circulation, and the suboptimal costimulation received at the tumor site are key reasons for the limited activity of chimeric antigen receptor-redirected T cells (CAR-Ts) in solid tumors. We have explored the benefits of incorporating the interleukin (IL)-15 cytokine within the CAR cassette to provide both a survival signal before antigen encounter, and an additional cytokine signaling at the tumor site using a neuroblastoma (NB) tumor model.

Experimental design: We optimized the construct for the CAR specific for the NB-antigen GD2 without (GD2.CAR) or with IL-15 (GD2.CAR.15). We then compared the expansion, phenotype and antitumor activity of T cells transduced with these constructs against an array of NB cell lines *in vitro* and *in vivo* using a xenogeneic metastatic model of NB.

Results: We observed that optimized GD2.CAR.15-Ts have reduced expression of the PD-1 receptor, are enriched in stem-cell like cells, and have superior antitumor activity upon repetitive tumor exposures *in vitro* and *in vivo* as compared to GD2.CAR-Ts. Tumor re-challenge experiments *in vivo* further highlighted the role of IL-15 in promoting enhanced CAR-Ts antitumor activity and survival, both in the peripheral blood and tissues. Finally, the inclusion of the inducible caspase-9 gene (iC9) safety switch warranted effective on demand elimination of the engineered GD2.CAR.15-Ts.

Conclusion: Our results guide new therapeutic options for GD2.CAR-Ts in patients with NB, and CAR-T development for a broad range of solid tumors.

3

INTRODUCTION

Neuroblastoma (NB) is the most common extracranial tumor of childhood[1]. Since children with high-risk NB continue to have poor outcome despite intensive chemotherapy regimens, new treatment strategies are required[2, 3]. The disialoganglioside GD2, which is consistently expressed in NB tumor cells with restricted expression in normal tissues, represents the target of choice for immunotherapy in NB, through either a specific monoclonal antibody (Ch14.18, dinutuximab) or, more recently, chimeric antigen receptor engineered T cells (GD2.CAR-Ts)[3-6].

In the first clinical study with GD2.CAR-Ts, the specific scFv was derived from the murine 14.G2a monoclonal antibody coupled with the ζ-chain endodomain (1st generation CAR), and engrafted in Epstein-Barr-virus-specific cytotoxic T lymphocytes[5, 6]. In the second clinical trial, the same CAR was modified to encode two costimulatory endodomains in tandem (CD28 and OX40) (3rd generation CAR) and expressed in polyclonal T lymphocytes[4]. Both studies showed that infusions of GD2.CAR-Ts were well tolerated, even when combined with conditioning regimens to lymphodeplete the host, and promoted some objective clinical responses[4-6].

However, response rates in NB patients receiving GD2.CAR-Ts remain significantly inferior to those observed in patients with acute lymphoblastic leukemia treated with CD19-specific CAR-Ts[7]. It is also evident that, while the inclusion of costimulatory endodomains like CD28 or 4-1BB in the CD19-specific CAR is necessary and sufficient to achieve clinical responses[7-11], CAR costimulation is not equally effective in NB[4]. Furthermore, while the expansion of CD19-specific CAR-Ts in the peripheral blood correlates with clinical responses[7], increases of GD2.CAR-Ts in the peripheral blood, even when these cells are infused in lymphodepleted patients, do not promote better antitumor responses[4]. We speculated that, despite

4

homeostatic expansion in peripheral blood, in contrast to CD19-specific CAR-Ts, GD2.CAR-Ts do not promptly receive the costimulation required for full activation while in the circulation, as they do not engage their cognate antigen. Furthermore, when GD2.CAR-Ts reach the tumor site, the costimulation provided through the signaling moieties of the CAR remains suboptimal to achieve complete elimination of tumor cells due to local inhibitory/suppressive factors. We observed here that the inclusion of the IL-15 cytokine within the CAR cassette is beneficial for GD2.CAR-Ts by promoting both enhanced survival in the absence of the cognate antigen, and prolonged antitumor activity.

5

MATERIALS AND METHODS

Cell lines. The NB cell lines IMR-32, LAN-1 and SKNLP were purchased from ATCC, while the CHLA255 cell line was previously described[12]. Cells were maintained in RPMI-1640 supplemented with 10% fetal bovine serum and 2 mmol/L L-glutamine (Invitrogen). Tumor cell lines were transduced with a gamma retroviral vector encoding the enhanced GFP (eGFP) or the Firefly-Luciferase (FFLuc) genes as previously described [13]. Cells were routinely (monthly) screened for the presence of mycoplasma and expression of the GD2 antigen and kept in culture for less than 3 consecutive months, after which aliquots from the original expanded vial were used.

Plasmid and retrovirus construction. The cassette encoding the GD2 specific scFv (scFv14G2a), the CD8α stalk and transmembrane domain, the CD28 intracellular domain and CD3ζ chain was cloned into the SFG backbone (GD2.CAR). The scFv14G2a was previously identified[14] and used in clinical studies[4-6]. We modified this scFv14G2a by removing 16 amino acids from the COOH-region of the V_H (AKTTPPSVYGRVYVSS). Indeed, when we aligned the previously used V_H sequence into the IGBLAST NCBI database, these 16 amino acids, which belong to the CDR3-IMGT (germline) of the V_H, exceeded the alignment of the V_H sequence reported in the dataset. Furthermore, two versions of the scFv14G2a were produced by conserving the previously used 9-aminoacid linker (SL) between the V_L and V_H fragments or including a 20-aminoacid linker (LL). We then generated vector cassettes encoding the CAR in combination with the IL-15 *cdna* (GD2.CAR.15) using a 2A-sequence peptide[15]. In a third vector, we also cloned the inducible caspase-9 suicide gene[16] into the GD2.CAR.15 using a second 2A-sequence peptide (iC9.GD2.CAR.15). Finally, for selected experiments, the scFv14G2a in the iC9.GD2.CAR.15 vector was swapped with the CD19-specific scFv[17] to obtain the iC9.CD19.CAR.IL-15 vector. Vectors encoding the Firefly-luciferase (FFluc) and the fusion protein GFP have been previously described[13]. The full-length human PD-L1

6

(accession_NM_014143.4) was PCR amplified, cloned into the retroviral vector SFG and used to transduce the CHLA255 tumor cell line to generate tumor cells constitutively expressing high levels of PD-L1 (CHLA255-PD-L1[+]). Transient retroviral supernatants were produced as previously described[13]. For GMP translation and validation studies a clinical grade packaging cell line was generated by using the PG13 packaging cell line (gibbon ape leukemia virus pseudotyping packaging cell line; CRL-10686, ATCC) as previously described[5]. We used the highest-titer clone to establish the master cell bank as recommended by FDA guidelines.

Generation of CAR-Ts. Peripheral blood mononuclear cells (PBMCs) were isolated from buffy coats (Gulf Coast Regional Blood Center) using Lymphoprep (Accurate Chemical and Scientific Corporation). PBMCs were then activated using 1 µg/mL immobilized CD3 (Miltenyi Biotech) and CD28 (BD Biosciences) monoclonal antibodies (mAbs). After 3 days, cells were transduced with retroviral supernatants and expanded in complete medium (45% RPMI-1640 and 45% Click's medium, 10% FBS, and 2 mM GlutaMAX) supplemented with IL-7 (10 ng/mL, PeproTech) and IL-15 (5 ng/mL, PeproTech) and expanded by feeding them every 3 - 4 days with fresh complete media and cytokines, as previously described[18-20].

Western Blot analysis. T cell lysates were resuspended in 2x Laemelli Buffer (BioRad) in reducing (with β-mercaptoethanol) or non-reducing (without β-mercaptoethanol) conditions. All lysates were separated in 4-15% sodium dodecyl sulfate polyacrylamide (SDS-PAGE) gels and transferred to polyvinylidene diflouride membranes (all BioRad). Blots were probed for human CD3ζ Ab (Santa Cruz Biotechnology, Dallas, TX) diluted 1:1000 in TBS-Tween/5% skim milk. Membranes were then incubated with HRP-conjugated goat α-mouse or goat α-rabbit IgG (both Santa Cruz) at a dilution of 1:3000 and imaged using the ECL Substrate Kit on a ChemiDoc MP System (both BioRad) according to manufacturer's instructions.

Co-culture experiments. eGFP-transduced tumor cells were plated in 24-well plates at a concentration of 0.25 or 0.5 × 10^6 cells/well the day before the addition of T cells, in the absence of cytokines. Different effector cells to target cells (E:T) ratios were used (1:1, 1:5 and 1:10). For the repetitive co-culture experiments, T cells and eGFP-tagged NB cells were co-cultured at the E:T ratio of 1:1 or 1:5. At day 3, all cells were transferred into a new well and seeded with 0.25 × 10^6 NB cells. T cells and NB cells were quantified by flow cytometry after 4 cycles based on CD3 and GFP expression, respectively. Supernatant were also collected for cytokine measurements after each cycle. For each experiment non-transduced T cells were used as a negative control (Ctrl-Ts).

Carboxyfluorescein succinimidyl ester (CFSE)-based proliferation assay. CAR-Ts and control T cells were labeled with CFSE (Invitrogen) and plated in the wells precoated with or without the 1A7 antibody (0.5 μg/well). On day 5, cells were collected and analyzed for CFSE dilution by flow cytometry.

Side Population (SP) staining by Hoechst dye/Dye Cycle Violet and cell sorting. Cells were incubated in Hank's Balanced Salt Solution (Life Technologies) containing 2% FBS, 10 mM HEPES (Life Technologies), and either 10 μg/mL Hoechst 33342 (Sigma-Aldrich) for 90 min at 37°C. Cells were then washed with ice cold HBSS and labeled with CD3-APC for flow cytometry analysis. To detect the SP cells, Hoechst 33342 samples were excited using a 355nm UV laser on a LSRII/Fortessa flow cytometer (BD)[21, 22].

Cytokine measurements. Culture supernatants were collected after 24 hours of co-culture to measure the release of IL-2, IFN-γ and TNF-α, and after 72 hours for IL-15, using specific enzyme-linked immunosorbent assays (R&D systems, Inc, Minneapolis, MN, USA). Plasma obtained from mice was analyzed for the presence of human cytokines using the Bio-Plex Pro™ Human Cytokine 8-plex Assay (Bio-Rad) or Human High Sensitivity Cytokine B Premixed Mag

8

Luminex Performance Assay (R&D) following manufacturer's instructions. Data were collected and analyzed using the Lumina-200 System and the Bio-Plex Manager 6.1 software (Bio-Rad).

Activation of the suicide gene. The B/B homodimerizer AP20187, a chemical inducer of dimerization drug (CID) (Clontech Laboratories), was added at 50 nM to T cell cultures and induction of apoptosis evaluated 24 hours later using Annexin-V/7AAD staining (BD Biosciences) and FACS analysis[16].

Immunophenotyping. Cells were acquired using the BD FACS Fortessa (BD Biosciences, North Ryde, Australia) and analyzed using the FlowJo Software (Tree Star, Ashland, OR). Monoclonal antibodies (Abs) specific for GD2, CD45, CD3, CD8, CD45RA, CD45RO, PD-1, CCR7, CD45, LAG-3, TIM-3, TIGIT, CTLA-4, CD25, CD69, active caspase-3 and granzymeB were obtained from BD Biosciences. To detect the GD2.CAR expression in transduced T cells, we used the 1A7 anti-idiotype mAb specific for the 14G2a.scFv and PE or APC-conjugated rat anti-mouse secondary mAbs (BD Biosciences)[5]. In selected experiments, counting beads (Count Bright, Invitrogen) were added following manufacture's instruction. For the intracellular staining, cells were stained with Zombie dye and surface antibodies, including CD3 and GD2, washed, fixed and permeabilized with Cytofix/Cytoperm (BD), and then stained with active caspase-3 in 1x permeabilization buffer, following manufacturer's instructions.

Xenogeneic neuroblastoma models. Mouse experiments were performed in accordance with the University of North Carolina (UNC) animal husbandry guidelines according to protocols approved by the UNC institutional animal care and use committee. For these studies, 6 - 8 weeks old female and male NSG mice (NOD.Cg-$Prkdc^{scid}$ $IL2$rg^{tm1Wj1}/SzJ, UNC Animal Studies Core Facility) received intravenously via tail injection (i.v.) 2×10^6 CHLA255 cells labeled with FFLuc. Tumor engraftment was measured as bioluminescence signal intensity (BLI) and expressed as total flux (p/s) using the *in vivo* IVIS imaging (Caliper Life Science)[23]. Two

9

weeks after tumor engraftment, mice received i.v. either 2×10^6, 5×10^6 or 10×10^6 control-Ts (Ctrl) or CAR-Ts. No exogenous cytokines were administered to the mice. Mice were bled at specific intervals (10 - 15 days, as per UNC-IACUC guidelines) to measure cytokines in the plasma and frequency of CAR-Ts. Mice were followed after CAR-Ts treatment and euthanized when tumor growth caused discomfort as per veterinarian's recommendation. At the time of euthanasia, blood, spleen, liver and bone marrow were isolated and analyzed to detect CAR-Ts. To assess differences in response to continuous exposure to tumor cells, we performed tumor re-challenge experiments, where tumor-bearing mice were further injected i.v. with 3×10^6 CHLA255 cells labeled with FFLuc at day 7 and 14 or at day 28 after CAR-T treatment. In selected experiments, tumor bearing mice received i.p. the PD-1 blocking antibody (clone EH12.2H7, Biolegend) (200 µg per mouse every 4 days) starting from the day before the CAR-Ts infusion. In some experiments, mice were engrafted with the FFLuc CHLA255 tumor cell line genetically engineered to express high levels of PD-L1 (CHLA255-PD-L1$^+$ cells) in the attempt to further promote T cell exhaustion *in vivo.* To ensure the function of the suicide gene, 10×10^6 FFLuc-tagged CAR-Ts were injected i.v. into NSG mice. T cell expansion was then tracked by *in vivo* imaging measuring T-cell BLI. Mice were randomized to receive vehicle or CID (AP20187, 50 µg/mouse), and then imaging was performed to evaluate the elimination of T cells. In selected experiments, mice were challenged with 3×10^6 CHLA255 cells, 4 days after CID/vehicle treatment.

Statistical analysis. ANOVA with Bonferroni correction and the 2-sided unpaired t test were used for comparison of 3 or more groups, or 2 groups, respectively, as stated in the figure legends. Mixed model ANOVA was applied to compare tumor growth in different groups of mice. Survival curves were plotted using the Kaplan-Meier method, and the differences in the survival between groups were assessed by log-rank test. Data are presented as mean ± SD or SEM as

10

stated in the figure legends. Statistical significance was defined at P<0.05. Statistical analysis

was performed with Prism 5 (GraphPad Software).

11

RESULTS

T lymphocytes transduced with a modified GD2.CAR expressing the IL-15 retain a central memory/stem-cell-like phenotype and show lower expression of inhibitory receptors. We first reevaluated the structure of the GD2.CAR generated using the scFv derived from the 14G2a mAb. Specifically, we compared the previously constructed GD2.CARs encoding the CD28 endodomain[24] with a modified GD2.CAR, characterized by a shortened V_H sequence and containing the hinge and transmembrane domain of human CD8α instead of the Ig-derived hinge and CD28 transmembrane domain, and found that the new optimized GD2.CAR had superior activity in *in vitro* experiments (**Fig.S1A-F**), and reduced self-dimerization (**Fig.S1G**). We then generated two cassettes, encoding either the optimized GD2.CAR alone or the GD2.CAR in combination with IL-15 (GD2.CAR.15) using a 2A-sequence peptide (**Fig.1A**). CAR expression (**Fig.1B**) and expansion (**Fig.1C**) of T cells transduced with either GD2.CAR or GD2.CAR.15 vectors were similar. Phenotypically both GD2.CAR-Ts and GD2.CAR.15-Ts contained similar amounts of CD4$^+$ and CD8$^+$ T cells (**Fig.S2A**). In contrast, GD2.CAR.15-Ts contained higher frequency of central-memory T cells (CD45RO$^+$CCR7$^+$) (15% ± 7% vs. 7% ± 3%, p<0.01) and stem-cell like T cells (CD45RA$^+$CCR7$^+$) (25% ± 11% vs. 6% ± 2%, p<0.001) than GD2.CAR-Ts (**Fig.1D**). Furthermore, GD2.CAR.15-Ts showed lower constitutive expression of PD-1 as compared to GD2.CAR-Ts in both central-memory (25% ± 20% vs. 39% ± 17%, p<0.001) and stem-cell like T cells (8% ± 11% vs. 17%± 14%, p<0.01) (**Fig.1E** and **Fig.S2B**). Down-regulation of PD-1 in GD2.CAR.IL-15-Ts was confirmed at the transcription level (**Fig.S2C**). In GD2.CAR.IL-15-Ts we also observed low expression of another inhibitory receptor, namely LAG-3 (**Fig.S2D**), while the activation markers CD25 and CD69 were equally expressed in GD2.CAR-Ts and GD2.CAR.IL-15-Ts (**Fig.S2E**). Susceptibility to activation induced cell death (AICD) was also comparable between GD2.CAR-Ts and GD2.CAR.15-Ts (**Fig.S2F**). Overall these data suggest that the low expression of PD-1 and LAG-3 in

12

GD2.CAR.IL-15-Ts does not reflect lower activation but rather a superior fitness. These data were corroborated in experiments showing that GD2.CAR.15-Ts proliferated and persisted longer in the absence of exogenous cytokines or antigen support *in vitro* (**Fig.S2G**) and in vivo (**Fig.S3A,B**), mimicking the advantage they will have in the circulation before engaging tumor cells.

GD2.CAR.15-Ts have improved antitumor activity and expansion upon antigen exposure *in vitro*. We co-cultured GD2.CAR-Ts and GD2.CAR.15-Ts with four NB cell lines (including MYCN-amplified NB cells) at an E:T ratio of 1:1 (**Fig.S4A**). Both GD2.CAR-Ts and GD2.CAR.15-Ts efficiently eliminated tumor cells (**Fig.2A** and **Fig.S4B**), including putative tumor stem cells identified as SP cells (**Fig.S4C**). However, GD2.CAR.15-Ts proliferated significantly better in response to all NB cell line tested (**Fig.2B**). IL-15 was detectable in the supernatant of co-cultures with GD2.CAR.15-Ts, while no significant differences were observed for other cytokines, including IL-2, TNF-α and IFN-γ or granzymeB release as compared to GD2.CAR-Ts (**Fig.2C and Fig.S4D,E**). Moreover, as observed during the *in vitro* expansion with cytokines, without antigen stimulation, GD2.CAR.15-Ts showed lower expression of PD-1 (**Fig.2D**) and LAG-3 (**Fig. S4F**) upon co-culture with NB cells as compared to GD2.CAR-Ts. Target cells showed the same level of cleaved caspase-3, which is another marker of apoptosis, 24 hours post co-culture (**Fig.S4G**) indicating similar kinetic of cytotoxic activity of GD2.CAR-Ts and GD2.CAR.IL15-Ts. Remarkably, GD2.CAR.15-Ts showed sustained antitumor activity in stress co-culture experiments[25] in which T cells were repetitively exposed to antigen engagement using CHLA255 and LAN-1 cells (**Fig.S5A**). After 4 cycles of co-culture, GD2.CAR.15-Ts, but not GD2.CAR-Ts, significantly controlled tumor growth of both CHLA255 and LAN-1 cells (p<0.05 and p<0.01, respectively) (**Fig.2E and Fig.S5B**) and proliferated in response to repetitive exposure to each respective tumor cell line (p<0.01 and p<0.05, respectively) (**Fig.2F**). GD2.CAR.15-Ts continued to produce IL-15 after each cycle of

13

stimulation in response to both CHLA255 (**Fig.2G**) and LAN-1 (**Fig.S5C**) cells. IFN-γ was released by CAR-Ts independently of the IL-15 expression after the second round of stimulation with CHLA255 cells (**Fig.S5D**), and upon repetitive antigen exposure, GD2.CAR.15-Ts continued to show lower PD-1 expression as compared to GD2.CAR-Ts (**Fig.2H**). As observed after repetitive exposures to the tumor cells, CD25 and CD69 expression were similar between GD2.CAR-Ts and GD2.CAR.IL15-Ts (**Fig.S5E**), and similar AICD was observed (**Fig.S5F**). Overall, transgenic expression of IL-15 harnessed significantly superior antitumor activity in an antigen dependent fashion by promoting sustained T cell proliferation after multiple exposures to tumor cells.

GD2.CAR.15-Ts are protective in an _in vivo_ tumor re-challenge model. We compared the antitumor activity of GD2.CAR-Ts and GD2.CAR.15-Ts in a metastatic NB model using NSG mice engrafted with the CHL255 NB tumor cell line (**Fig.3A**). At the time of T cell infusion mice were randomized based on the tumor BLI to ensure similar tumor burden between the experimental groups (**Fig. S6A**). Tumor grew rapidly in mice treated with Ctrl cells, while GD2.CAR-Ts and GD2.CAR.15-Ts promoted equal control of tumor growth at day 50 when 1 x 10^7 T cells/mouse were infused (**Fig.3B**). In contrast, only GD2.CAR.15-Ts succeeded in controlling tumor growth at day 50 when 5 x 10^6 T cells/mouse or 2 x 10^6 T cells/mouse were infused (**Fig.3C,D**). The protective effect of GD2.CAR.15-Ts was even more prominent in tumor re-challenge experiments, when mice, in addition to the initial tumor burden, received weekly infusions of NB tumor cells (**Fig.4A**). GD2.CAR.15-Ts treated mice were tumor free >50 days post T-cell infusion, while tumor growth was evident 2 weeks after the 1st tumor re-challenge in mice treated with GD2.CAR-Ts (**Fig.4B-D**). GD2.CAR.15-Ts were detectable in the peripheral blood, and, consistently with the _in vitro_ data, showed lower PD-1 expression (**Fig.4E**). GD2.CAR.15-Ts were also detected in bone marrow, liver and spleen at the time of euthanasia (**Fig.4F**) and showed low PD-1 expression, although in these later stages they were mostly

14

effector cells (CD45RO⁺CD45RA⁻CCR7⁻) (**Fig.S6B-D**). In addition to IFN-γ, IL-15 produced by

GD2.CAR.15-Ts was detectable in the plasma up to day 23 post infusion (**Fig.4G**), while IL-2

and TNF-α were below the limit of detection (**Fig.S6E**). To investigate whether the decreased

PD-1 expression in GD2.CAR.15-Ts protects these cells *in vivo* from tumor induced exhaustion,

tumor bearing mice were treated with GD2.CAR-Ts or GD2.CAR.15-Ts in combination with the

PD-1 blocking Ab (**Fig.S7A**). PD-1 blockade did not provide any advantage in mice treated with

GD2.CAR.15-Ts, since these cells show low PD-1 expression (**Fig.S7B**). However, we also

found that PD-1 blockade did not significantly improve persistence, cytokine release

(**Fig.S7C,D**) and antitumor activity (**Fig.S7B**) in mice treated with CAR.GD2-Ts. When we used

CHLA255 cells constitutively expressing PD-L1 (**FigS8A**), GD2.CAR.15-Ts cells continued to

control tumor growth with or without PD-1 blockade, while a modest advantage was observed

with PD-1 blockade in mice treated with GD2.CAR-Ts (**Fig.S8B-D**). These data indicate that

GD2.CAR.15-Ts persist better after tumor clearance and after tumor re-challenge, but these

effects are not directly correlated with an improved resistance to PD-L1 inhibition.

An optimized GD2.CAR construct allows the accommodation of the iC9 safety switch, while preserving the functionality of IL-15. Because of the potential for aberrant T-cell

proliferation or toxicities in the presence of sustained exposure to IL-15, we included the iC9

safety switch gene into our construct, to promptly remove GD2.CAR.15-Ts. Upon inclusion of

the iC9 *cdna* into the GD2.CAR.15 cassette, we unexpectedly observed a progressive loss of

CAR expression when cells were maintained in culture, with a consequent reduced antitumor

activity *in vit*ro (**Fig.S9A**). This phenomenon was a unique feature of the GD2.CAR, as a similar

cassette constructed to express the CD19-specific CAR did not show any significant reduction

of the CAR expression (**Fig.S9B**). Since the only difference in the two scFvs (CD19-specific and

GD2-specific) was the size of the linker (20 versus 9 amino acids, respectively) we replaced the

short-linker in the GD2-specific scFv with a long-linker (**Fig.S9C**). While the size of the linker did

15

not significantly affect the expression and function of the GD2.CAR in the absence of the iC9 (**Fig.9D-F**), the long-linker stabilized the GD2.CAR expression when the iC9 *cdna* was incorporated within the cassette (iC9.GD2.CAR.15) (**Fig.S10A, B**), allowing proper T cell expansion *in vitro* (**Fig.S10C**), and preservation of the same cell subset composition (**Fig.S10D**). Expanded iC9.GD2.CAR.15-Ts showed functional activity of all three genes incorporated within the cassette. Specifically, the inclusion of the iC9 caused cell death when iC9.GD2.CAR.15-Ts were incubated with 50 nM of the CID/AP20187 (**Fig.S10E**). Moreover, iC9.GD2.CAR.15-Ts showed *in vitro* anti-tumor activity, proliferative capacity against CHLA255 or LAN-1 cells comparable to that of GD2.CAR.15-Ts (**Fig.S10F** and **Fig.S11A,B**), similar pattern of PD-1 expression (**Fig.S10G** and **Fig.S11C**), and similar release of cytokines (**Fig.S10H** and **Fig.S11D**). Overall, an optimal design of the GD2.CAR allowed the functional accommodation of both the IL-15 and iC9 transgenes.

Using our re-challenge tumor model, we finally assessed *in vivo* the antitumor effects of iC9.GD2.CAR.15-Ts (**Fig.5A**). While tumor BLI rapidly increased in the control group, mice treated with GD2.CAR.15-Ts and iC9.GD2.CAR.15-Ts remained tumor free by day 40 post re-challenge (**Fig.5B, C**). This translated in a significantly better tumor free survival (p<0.0001) (**Fig.5D**). GD2.CAR.15-Ts and iC9.GD2.CAR.15-Ts showed similar persistence (**Fig.5E**) in mice after infusion, without significant differences in T cell composition (**Fig.S12A**). Together, our data show that the incorporation of the iC9 safety switch into an optimized GD2.CAR.15 construct remains beneficial *in vivo*.

To validate the functionality of the iC9 suicide gene, NSG mice infused i.v. with eGFP-FFLuc labeled iC9.GD2.CAR.15-Ts were treated with either AP20187 (CID) (50 μg/mouse) or diluent (vehicle) (**Fig.6A**). While progressively increasing in mice treated with vehicle, BLI decreased promptly and remained low after CID administration (**Fig.6B**). Similarly, phenotypic analysis showed that circulating human T cells almost completely disappeared in CID-treated mice, while increased in vehicle-treated mice (2% ± 0.5% vs. 25%± 2%, p< 0.001) (**Fig.6C**). When we

16

analyzed tissues collected at the end of the observation period, CAR-Ts were reduced in CID-treated mice as compared to vehicle-treated mice (**Fig.6D**). Finally, in selected experiments when mice were re-challenged with tumor cells after CID or vehicle treatment to reactivate residual T cells, we observed no increase in BLI in any of the mice that previously received CID (**Fig.6E**), which suggests that the residual CAR-Ts after CID treatment are not reactivated and thus cannot cause toxicity *in vivo*.

To further demonstrate the clinical applicability of the proposed approach we have generated a clinical grade PG13 retroviral packaging cell line[20] and produced clinical grade supernatant. As shown in **Fig.S13**, iC9.GD2.CAR.15-Ts generated under GMP conditions for clinical use maintained the same characteristic of those generated in preclinical experiments ensuring the clinical application of the proposed strategy in patients with NB. The clinical protocol was recently approved by FDA (IND 18500).

17

DISCUSSION

GD2.CAR-Ts expressing costimulatory endodomains have been proven safe in patients with NB, but their antitumor activity remains limited[4], suggesting that additional preclinical assessment is needed to improve their clinical activity. Here we show that modifications of the GD2.CAR structure and the incorporation of IL-15 proved to be key requirements to enhance antitumor activity without causing on target toxicity.

Our rationale for redesigning GD2.CAR-Ts stems from both laboratory and clinical observations. Laboratory observations have highlighted how structural characteristics of CAR molecules, such as the framework regions of the scFv, and the length and origin of the hinge, and of the transmembrane endodomain, can impact the functionality of CAR-Ts[26-28]. Specifically for the scFv of the GD2.CAR obtained from the 14g2a Ab, high tendency for self-aggregation secondary to interactions within the scFv framework regions has been described[27]. This phenomenon was associated to an overstimulation of GD2.CAR-Ts, resulting in the premature exhaustion and reduced antitumor activity of these cells when the CAR contained the CD28 costimulatory signal[27]. Furthermore, recent evidences indicated that a mutated version of the 14g2a.scFv (E101K), which enhances its binding affinity, although effective in controlling tumor growth, caused severe neurotoxicity in one study[29, 30], but not in another study[31]. On the other hand, in patients with B-cell derived malignancies the expansion of CD19-specific CAR-Ts in the peripheral blood correlates with objective antitumor activity[7]. In contrast GD2-specific CAR-Ts, although expanding in the peripheral blood when infused upon lymphodepletion, did not promote significant clinical benefits[4]. Based on these observations for the 14g2a-derived CAR, we sought to modify structural parts of our construct to address intrinsic limitations of the GD2.CAR cassette. In addition, we optioned for the inclusion of the IL-15 cytokine as a survival factor for GD2.CAR-Ts rather than relying simply on PIK3 and TRAF mediated signaling delivered by the combination of CD28 or OX40/4-1BB endodomains upon antigen encounter[24,

18

32-35]. We reasoned this would provide a cytokine signaling that is independent from the costimulation received, and from IL-2 that is released by CAR-Ts upon antigen engagement[32, 35]. We found that structural modifications of the GD2.CAR cassette reduced its spontaneous self-aggregation. Furthermore, upon incorporation of IL-15, GD2.CAR-Ts retained specificity, but showed enhanced expansion and antitumor activities *in vitro*, after repeated tumor exposures, and *in vivo* in our innovative xenograft solid tumor model, which includes multiple tumor cell re-challenges to recapitulate the high tumor burden in patients with solid tumors. Importantly, these effects were obtained without evidences of "on target off tumor" toxicities.

Our study highlights that the inclusion of IL-15 affords CAR.GD2-Ts with other important properties for translation into an effective therapy. First, the incorporation of the IL-15 within the GD2.CAR produced an enrichment of cells with "memory" and "stem-cell" like phenotypes. This occurred during the expansion culture period, was independent from the specific antigen encounter by CAR-Ts, and was significantly superior to that already provided by the addition of exogenous IL-15 and lL-7 cytokines in the culture[19, 36]. While the mechanistic explanation of this phenomenon requires further studies, the immediate implication of this observation is that IL-15 secreted by GD2.CAR-Ts promotes additional effects that are superior to those produced by soluble IL-15. This may also be critical in patients, as the IL-15 available in the plasma upon lymphodepletion, despite promoting T cell expansion, may be inferior to the IL-15 directly produced and released by GD2.CAR-Ts[4]. Exogenous administration of IL-15 is accompanied by systemic toxicities[37, 38], and thus we did not formally compare exogenous administration versus the endogenous production, as the former would not likely be clinically relevant. A membrane bound form of IL-15 expressed by CAR-Ts may be also beneficial [39]. However, the incorporation of this gene would compromise the expression and function of the CAR, as the construct exceeds the cargo capacity of one single vector.

19

As second advantage we observed is that GD2.CAR.15-Ts had significantly reduced expression of PD-1 and LAG-3 with and without antigen stimulation, and thus may be less susceptible to PD-L1-mediated inhibition, since NB cells can express PD-L1, either constitutively or upon exposure to IFN-γ (**Fig S8A**). The observed low expression of PD-1 and LAG-3 in GD2.CAR.IL-15-Ts is not related to a different activation status of these cells, but rather suggests their potential superior fitness upon multiple exposures to the antigen. The low expression of PD-1 in GD2.CAR.IL-15-Ts correlated *in vivo* with lack of additive effects with PD-1 blockade in controlling the tumor growth. Of note, in our xenograft model of NB, we also observed that PD-1 blockade did not improve the antitumor effects of GD2.CAR-Ts that express PD-1, and should be reinvigorated by PD-1 blockade. This outcome may be partially related to the murine model that does not allow sufficient time to establish T cell exhaustion. However, our data resemble the lack of activity we have previously reported in a pilot clinical trial in patients with NB[4]. Additional studies are needed to clearly assess if PD-1/PD-L1 blockade can have a positive effects when combined with GD2.CAR-Ts in NB. Nevertheless, our data indicate that GD2.CAR-Ts expressing IL-15 remain effective even in a model in which we caused constitutive expression of PD-L1 in NB cells.

Because IL-15 is a T cell growth cytokine, and GD2.CAR.IL-15-Ts have more "stem-ness" properties, we incorporated a safety switch for regulation of potential unwanted and uncontrolled expansion[16, 17, 40, 41]. Our data demonstrate that further CAR construction was required to functionally accommodate these three genes. However, upon optimization, the final vector cassette showed functionality *in vivo*, and we were able to scale up the production of the CAR-Ts for clinical use. This final step is important since complex CAR-T engineering strategies often fail to reach clinical applications due to difficulties in scaling up at GMP level the results obtained in preclinical experiments.

20

In conclusion, we demonstrate that GD2.CAR.15-Ts have functional properties that should provide enhanced antigen-independent persistence and improved antitumor activity. The clinical trial in patients with NB based on the proposed strategy will be performed in our institution (IND 18500) and if proven safe and effective it can have broader application for targeting solid tumors.

ACKNOWLEDGMENTS

FIGURE LEGEND

Figure 1. Expression of GD2.CAR in activated T cells. (A) Schematic representation of retroviral vectors encoding GD2.CAR with the CD28 endodomain with or without IL-15. (B) Flow cytometry histograms showing GD2.CAR expression in activated T cells for one representative experiment (left panel), and summary of all donors (right graph) (n=12). Non-transduced T cells or mock vector T cells were used as a control. (C) CAR-Ts expansion by day 11 after transduction (n=8). (D) Representative flow plots showing CD45RA, CD45RO, CCR7 and PD-1 expression in CAR-Ts collected at day 11 after transduction (left panel), and summary of all donors (right panel) (n=11). **P<0.01; ***P<0.001 by 2 way ANOVA test. (E) PD-1 expression in CD45RA and CCR7 subsets of CAR-Ts at day 11 after transduction (n=15). **P<0.01; ***P<0.001 by 2 way ANOVA test.

Figure 2. GD2.CAR-Ts producing IL-15 have enhanced cytotoxic activity upon repetitive exposure to tumor cells *in vitro* and produce Th1 cytokines. (A, B) Quantification of residual tumor cells (A), and enumeration of T cells (B) in co-cultures of control-Ts (Ctrl), GD2.CAR-Ts or GD2.CAR.15-Ts with four GD2$^+$ NB tumor cell lines (CHLA255, IMR32, LAN-1 and SKNLP) at the E:T ratio of 1:1 for 7 days (n=4). *P<0.05; ***P<0.001 by 2 way ANOVA test. (C) Cytokine released in the co-culture supernatant by Ctrl-Ts or CAR-Ts when co-cultured with CHLA255 cells at the E:T ratio of 1:1. IL-2, TNF-α and IFN-γ were detected in supernatant collected 24 hours after the culture, while IL-15 was detected after 72 hours (n=4). ***P<0.001 by 2 way ANOVA test. (D) PD-1 expression of Ctrl-Ts or CAR-Ts in culture with the indicated target cells at the E:T ratio of 1:1. Quantification of residual tumor cells (E) and enumeration of CAR-Ts (F) after four cycles of co-culture of GD2.CAR-Ts or GD2.CAR.15-Ts with CHLA255 or LAN-1 cells (n=10) at the E:T ratio of 1:1. *P<0.05; **P<0.01 by 2 way ANOVA test. (G) IL-15 released by GD2.CAR-Ts in response to CHLA255 cells after each cycle (n=3). *P<0.05 by 2 way ANOVA

22

test. (H) PD-1 expression by CAR-Ts after 4 cycles of co-culture with CHLA255 or LAN-1 cells at the E:T ratio of 1:1 (n=6). **P<0.01 by 2 way ANOVA test.

Figure 3. Transgenic IL-15 enhances antitumor effects of GD2.CAR-Ts *in vivo*. (A) Schematic representation of the metastatic xenograft NB model. NSG mice were inoculated intravenously (i.v.) via tail injection with 2×10^6 CHLA255 cells labeled with Firefly-luciferase and two weeks later received T cells i.v.. (B-D) Tumor growth in mice receiving 1×10^7 Ctrl-Ts or CAR-Ts (B), 5×10^6 Ctrl-Ts or CAR-Ts (C) or 2×10^6 Ctrl-Ts or CAR-Ts (D). Each panel shows images and bioluminescence (BLI) kinetics of tumor growth for each mouse (n=4-5/group).

Figure 4. Transgenic IL-15 promotes antitumor activity and persistence of GD2.CAR-Ts *in vivo* in a re-challenge tumor model. (A) Schematic representation of tumor re-challenge experiments in the metastatic xenograft NB model. After tumor engraftment and T-cell treatment, mice received i.v. tumor CHLA255 cells labeled with Firefly-luciferase (3×10^6 cells per mouse) on days 7 and 14. A group of mice infused with CHLA255 cells only was used as a second control for this model. (B) BLI illustrating tumor growth in mice. Arrows indicate the tumor re-challenges. (C) BLI kinetic of tumor growth. Each line represents an individual mouse for the Ctrl (n=5) or CAR-Ts treatment (n=5) and re-challenge group (n=2). Arrows indicate the tumor re-challenges. (D) Kaplan-Meier survival curve showing tumor free survival. Significance was determined by log rank test (Mantel-Cox). ***P = 0.0005. (E) Quantification of human T cells (CD45$^+$ cells) (upper panel) and CAR$^+$PD-1$^+$ cells (lower panel) in peripheral blood samples collected at days 7 and 14 post T cell infusion (n=5). *P<0.05; ***P<0.001 by 2 way ANOVA test. (F) Quantification of human T cells (CD45$^+$ cells) (upper panel) and CAR$^+$PD-1$^+$ cells (lower panel) in peripheral blood, bone marrow, liver and spleen at days 45 - 55 post T cell treatment (n=6). *P<0.05; **P<0.01; ***P<0.001 by 2 way ANOVA test. (G) Detection of IL-15

23

(left panel) and IFN-γ (right panel) in plasma samples collected at days 7, 14 and 23 post T cell treatment (n=5). **P<0.01 by 2 way ANOVA test.

Figure 5. iC9.GD2.CAR.15-Ts retain the same antitumor activity of GD2.CAR.IL15-Ts *in vivo*. (A) Schematic representation of tumor re-challenge experiments in a metastatic xenograft NB model. Upon tumor engraftment and T-cell treatment, mice received i.v. tumor CHLA255 cells labeled with Firefly-luciferase (3 x 10^6 cells per mouse) on days 7 and 14. A group of mice infused with CHLA255 cells alone was used as a second control for this model. (B) BLI illustrating tumor growth in mice. Arrows indicate the tumor re-challenges. (C) BLI kinetic of tumor growth. Each line represents an individual mouse. Arrows indicate the tumor re-challenge. (D) Kaplan-Meier survival curve showing tumor free survival. Significance was determined by log rank test (Mantel-Cox). ***P < 0.0001. (E) Quantification of human T cells (CD45$^+$ cells) (left panel) and CD3$^+$CAR$^+$ cells (right panel) in the peripheral blood of treated mice at days 10, 17 and 27 post T-cell infusions (n=5). **P<0.01 by 2 way ANOVA test.

Figure 6. iC9.GD2.CAR.15-Ts can be efficiently eliminated *in vivo* upon activation of the iC9 gene. (A) Schematic representation of the experiments in NSG mice to test the iC9 activity *in vivo*. NSG mice were inoculated i.v. with T cells labeled with Firefly-luciferase. Mice received the vehicle or CID via intraperitoneal injection. In additional experiments, mice were inoculated i.v. with CHLA-255 cells (3 x 10^6 cells per mouse) 4 days post CID with the aim to boost CAR-Ts that may have escaped CID-induced apoptosis. (B) Images from representative mice before and after receiving either vehicle or CID as indicated by the arrow. The graph shows the BLI for of iC9.GD2.CAR.15-Ts in mice treated with either vehicle of CID as indicated by the arrow (n=5). (C) Representative flow plots and summary of human CD45$^+$ and CAR$^+$ T cells in the peripheral blood before and after treatment with either vehicle or CID (n=5). (D) Summary of human CD45$^+$ and CAR$^+$ T cells in the peripheral blood and organs in the mice treated with either vehicle or CID (n=5). *P<0.05, ***P<0.001 by 2 way ANOVA test. (E) Images from representative mice

24

before and after receiving either vehicle or CID (gray arrow), and then re-challenged with tumor

cells (black arrow). The graph shows the BLI of iC9.GD2.CAR.15-Ts in mice treated with either

vehicle (n=4) or CID (n=5), and re-challenged with tumor cells.

Reference List

[1]   Maris JM. Recent advances in neuroblastoma. N Engl J Med 2010;362:2202-11.

[2]   Maris JM, Hogarty MD, Bagatell R, Cohn SL. Neuroblastoma. Lancet 2007;369:2106-20.

[3]   Yu AL, Gilman AL, Ozkaynak MF, et al. Anti-GD2 antibody with GM-CSF, interleukin-2, and isotretinoin for neuroblastoma. N Engl J Med 2010;363:1324-34.

[4]   Heczey A, Louis CU, Savoldo B, et al. CAR T Cells Administered in Combination with Lymphodepletion and PD-1 Inhibition to Patients with Neuroblastoma. Mol Ther 2017.

[5]   Pule MA, Savoldo B, Myers GD, et al. Virus-specific T cells engineered to coexpress tumor-specific receptors: persistence and antitumor activity in individuals with neuroblastoma. Nat Med 2008;14:1264-70.

[6]   Louis CU, Savoldo B, Dotti G, et al. Antitumor activity and long-term fate of chimeric antigen receptor-positive T cells in patients with neuroblastoma. Blood 2011;118:6050-6.

[7]   Maude SL, Frey N, Shaw PA, et al. Chimeric antigen receptor T cells for sustained remissions in leukemia. N Engl J Med 2014;371:1507-17.

[8]   Lee DW, Kochenderfer JN, Stetler-Stevenson M, et al. T cells expressing CD19 chimeric antigen receptors for acute lymphoblastic leukaemia in children and young adults: a phase 1 dose-escalation trial. Lancet 2015;385:517-28.

[9]   Brentjens RJ, Davila ML, Riviere I, et al. CD19-targeted T cells rapidly induce molecular remissions in adults with chemotherapy-refractory acute lymphoblastic leukemia. Sci Transl Med 2013;5:177ra38.

[10] Kochenderfer JN, Dudley ME, Kassim SH, et al. Chemotherapy-Refractory Diffuse Large B-Cell Lymphoma and Indolent B-Cell Malignancies Can Be Effectively Treated With Autologous T Cells Expressing an Anti-CD19 Chimeric Antigen Receptor. J Clin Oncol 2015;33:540-9.

[11] Savoldo B, Ramos CA, Liu E, et al. CD28 costimulation improves expansion and persistence of chimeric antigen receptor-modified T cells in lymphoma patients. J Clin Invest 2011;121:1822-6.

[12] Liu D, Song L, Wei J, et al. IL-15 protects NKT cells from inhibition by tumor-associated macrophages and enhances antimetastatic activity. J Clin Invest 2012;122:2221-33.

[13] Vera J, Savoldo B, Vigouroux S, et al. T lymphocytes redirected against the kappa light chain of human immunoglobulin efficiently kill mature B lymphocyte-derived malignant cells. Blood 2006;108:3890-7.

[14] Rossig C, Bollard CM, Nuchtern JG, Merchant DA, Brenner MK. Targeting of G(D2)-positive tumor cells by human T lymphocytes engineered to express chimeric T-cell receptor genes. Int J Cancer 2001;94:228-36.

26

[15]   Quintarelli C, Vera JF, Savoldo B, et al. Co-expression of cytokine and suicide genes to enhance the activity and safety of tumor-specific cytotoxic T lymphocytes. Blood 2007;110:2793-802.

[16]   Straathof KC, Pule MA, Yotnda P, et al. An inducible caspase 9 safety switch for T-cell therapy. Blood 2005;105:4247-54.

[17]   Diaconu I, Ballard B, Zhang M, et al. Inducible Caspase-9 Selectively Modulates the Toxicities of CD19-Specific Chimeric Antigen Receptor-Modified T Cells. Mol Ther 2017;25:580-92.

[18]   Ramos CA, Ballard B, Zhang H, et al. Clinical and immunological responses after CD30-specific chimeric antigen receptor-redirected lymphocytes. J Clin Invest 2017;127:3462-71.

[19]   Xu Y, Zhang M, Ramos CA, et al. Closely related T-memory stem cells correlate with in vivo expansion of CAR.CD19-T cells and are preserved by IL-7 and IL-15. Blood 2014;123:3750-9.

[20]   Ramos CA, Savoldo B, Torrano V, et al. Clinical responses with T lymphocytes targeting malignancy-associated kappa light chains. J Clin Invest 2016;126:2588-96.

[21]   Hirschmann-Jax C, Foster AE, Wulf GG, et al. A distinct "side population" of cells with high drug efflux capacity in human tumor cells. Proc Natl Acad Sci U S A 2004;101:14228-33.

[22]   Hong LK, Chen Y, Smith CC, et al. CD30-Redirected Chimeric Antigen Receptor T Cells Target CD30(+) and CD30(-) Embryonal Carcinoma via Antigen-Dependent and Fas/FasL Interactions. Cancer Immunol Res 2018;6:1274-87.

[23]   Nishio N, Diaconu I, Liu H, et al. Armed oncolytic virus enhances immune functions of chimeric antigen receptor-modified T cells in solid tumors. Cancer Res 2014;74:5195-205.

[24]   Pule MA, Straathof KC, Dotti G, Heslop HE, Rooney CM, Brenner MK. A chimeric T cell antigen receptor that augments cytokine release and supports clonal expansion of primary human T cells. Mol Ther 2005;12:933-41.

[25]   Hoyos V, Savoldo B, Quintarelli C, et al. Engineering CD19-specific T lymphocytes with interleukin-15 and a suicide gene to enhance their anti-lymphoma/leukemia effects and safety. Leukemia 2010;24:1160-70.

[26]   Hudecek M, Lupo-Stanghellini MT, Kosasih PL, et al. Receptor affinity and extracellular domain modifications affect tumor recognition by ROR1-specific chimeric antigen receptor T cells. Clin Cancer Res 2013;19:3153-64.

[27]   Long AH, Haso WM, Shern JF, et al. 4-1BB costimulation ameliorates T cell exhaustion induced by tonic signaling of chimeric antigen receptors. Nat Med 2015;21:581-90.

[28]   Geldres C, Savoldo B, Dotti G. Chimeric antigen receptor-redirected T cells return to the bench. Semin Immunol 2016;28:3-9.

27

[29] Richman SA, Nunez-Cruz S, Moghimi B, et al. High-Affinity GD2-Specific CAR T Cells Induce Fatal Encephalitis in a Preclinical Neuroblastoma Model. Cancer Immunol Res 2018;6:36-46.

[30] Richman SA, Milone MC. Neurotoxicity Associated with a High-Affinity GD2 CAR-Response. Cancer Immunol Res 2018;6:496-7.

[31] Majzner RG, Weber EW, Lynn RC, Xu P, Mackall CL. Neurotoxicity Associated with a High-Affinity GD2 CAR-Letter. Cancer Immunol Res 2018;6:494-5.

[32] Dotti G, Gottschalk S, Savoldo B, Brenner MK. Design and development of therapies using chimeric antigen receptor-expressing T cells. Immunol Rev 2014;257:107-26.

[33] Imai C, Mihara K, Andreansky M, et al. Chimeric receptors with 4-1BB signaling capacity provoke potent cytotoxicity against acute lymphoblastic leukemia. Leukemia 2004;18:676-84.

[34] Finney HM, Akbar AN, Lawson AD. Activation of resting human primary T cells with chimeric receptors: costimulation from CD28, inducible costimulator, CD134, and CD137 in series with signals from the TCR zeta chain. J Immunol 2004;172:104-13.

[35] Sadelain M, Brentjens R, Riviere I. The basic principles of chimeric antigen receptor design. Cancer Discov 2013;3:388-98.

[36] Cieri N, Camisa B, Cocchiarella F, et al. IL-7 and IL-15 instruct the generation of human memory stem T cells from naive precursors. Blood 2013;121:573-84.

[37] Berger C, Berger M, Hackman RC, et al. Safety and immunologic effects of IL-15 administration in nonhuman primates. Blood 2009;114:2417-26.

[38] Conlon KC, Lugli E, Welles HC, et al. Redistribution, hyperproliferation, activation of natural killer cells and CD8 T cells, and cytokine production during first-in-human clinical trial of recombinant human interleukin-15 in patients with cancer. J Clin Oncol 2015;33:74-82.

[39] Hurton LV, Singh H, Najjar AM, et al. Tethered IL-15 augments antitumor activity and promotes a stem-cell memory subset in tumor-specific T cells. Proc Natl Acad Sci U S A 2016;113:E7788-E7797.

[40] Di Stasi A., Tey SK, Dotti G, et al. Inducible apoptosis as a safety switch for adoptive cell therapy. N Engl J Med 2011;365:1673-83.

[41] Zhou X, Dotti G, Krance RA, et al. Inducible caspase-9 suicide gene controls adverse effects from alloreplete T cells after haploidentical stem cell transplantation. Blood 2015;125:4103-13.
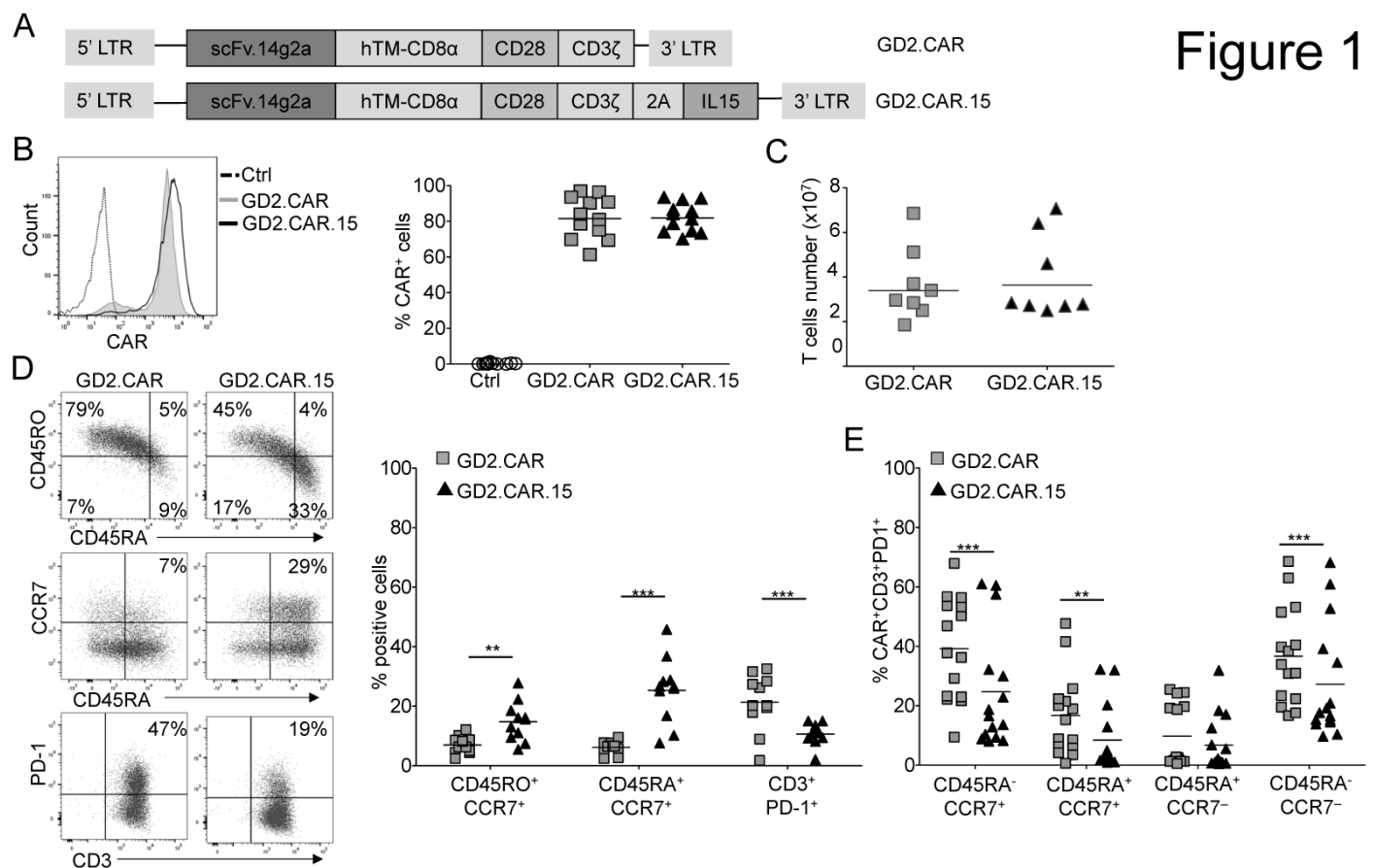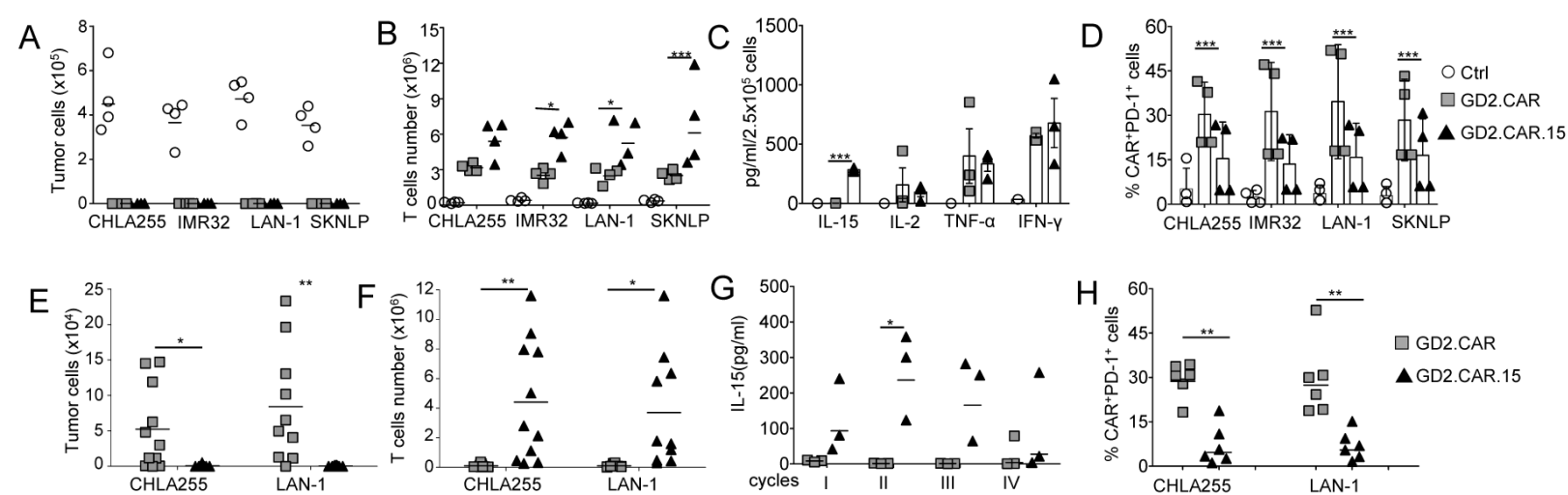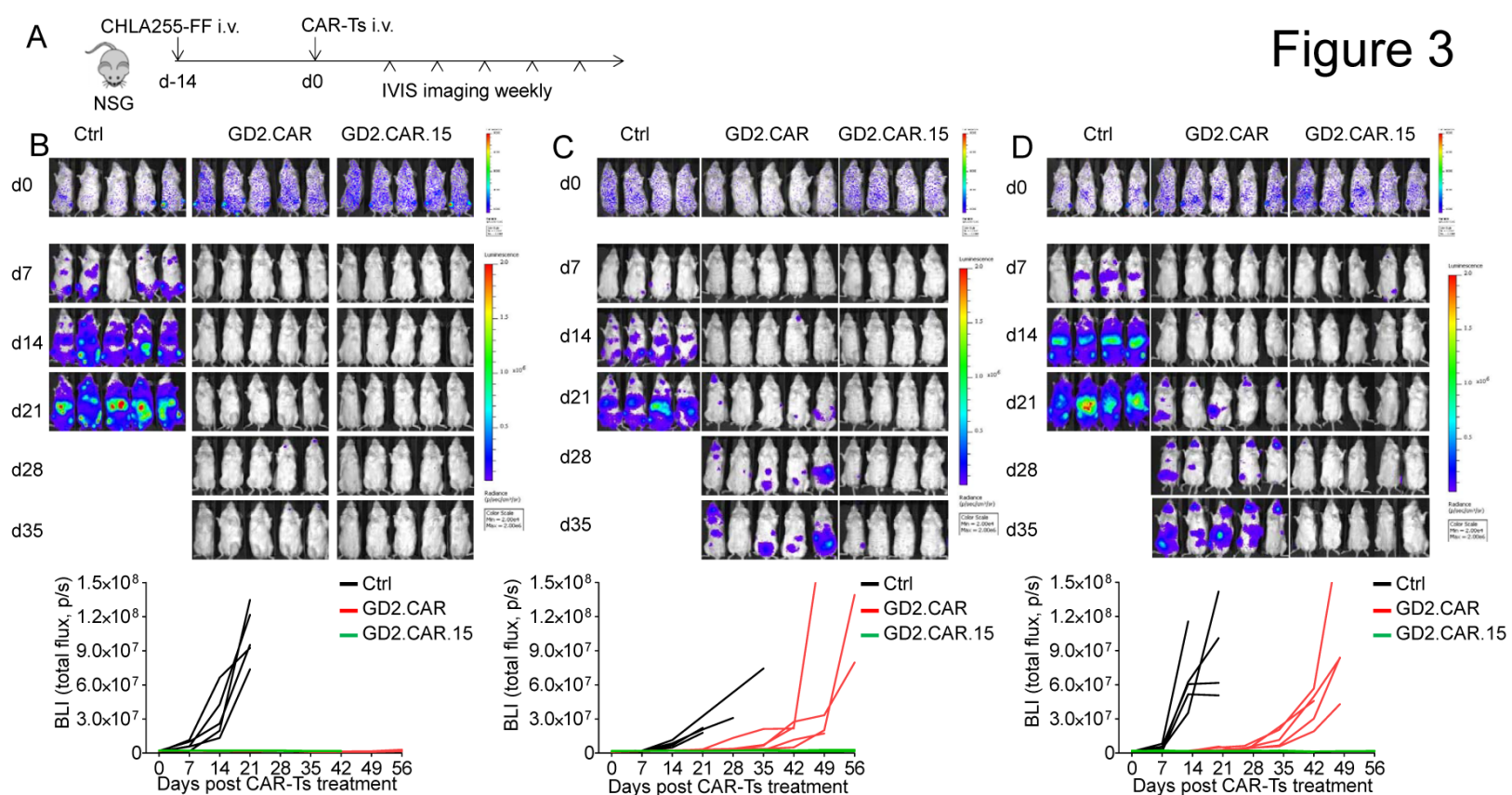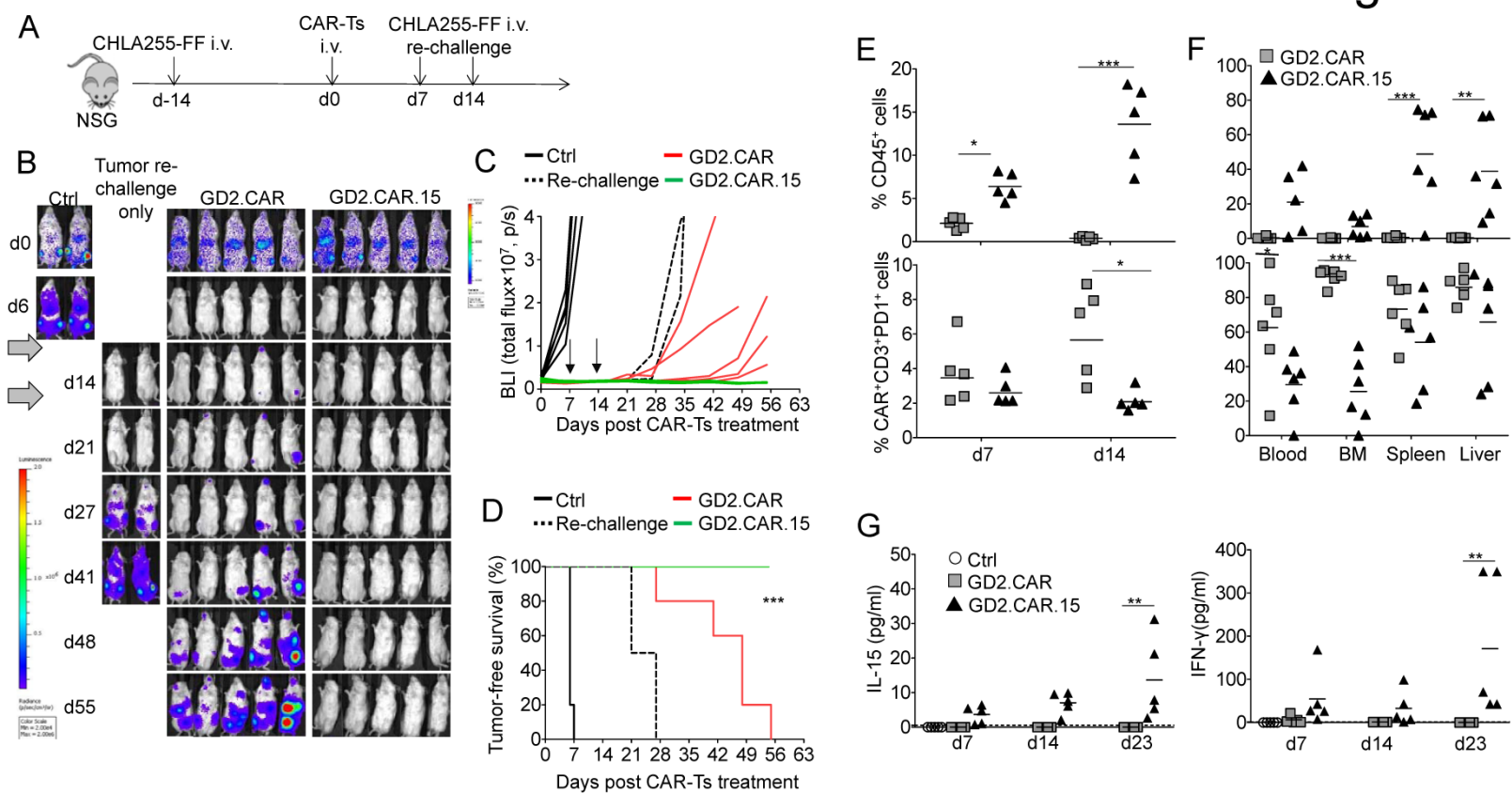
28

Figure 1

Figure 2

Figure 3

Figure 4

Figure 5

Figure 6

AACR American Association for Cancer Research
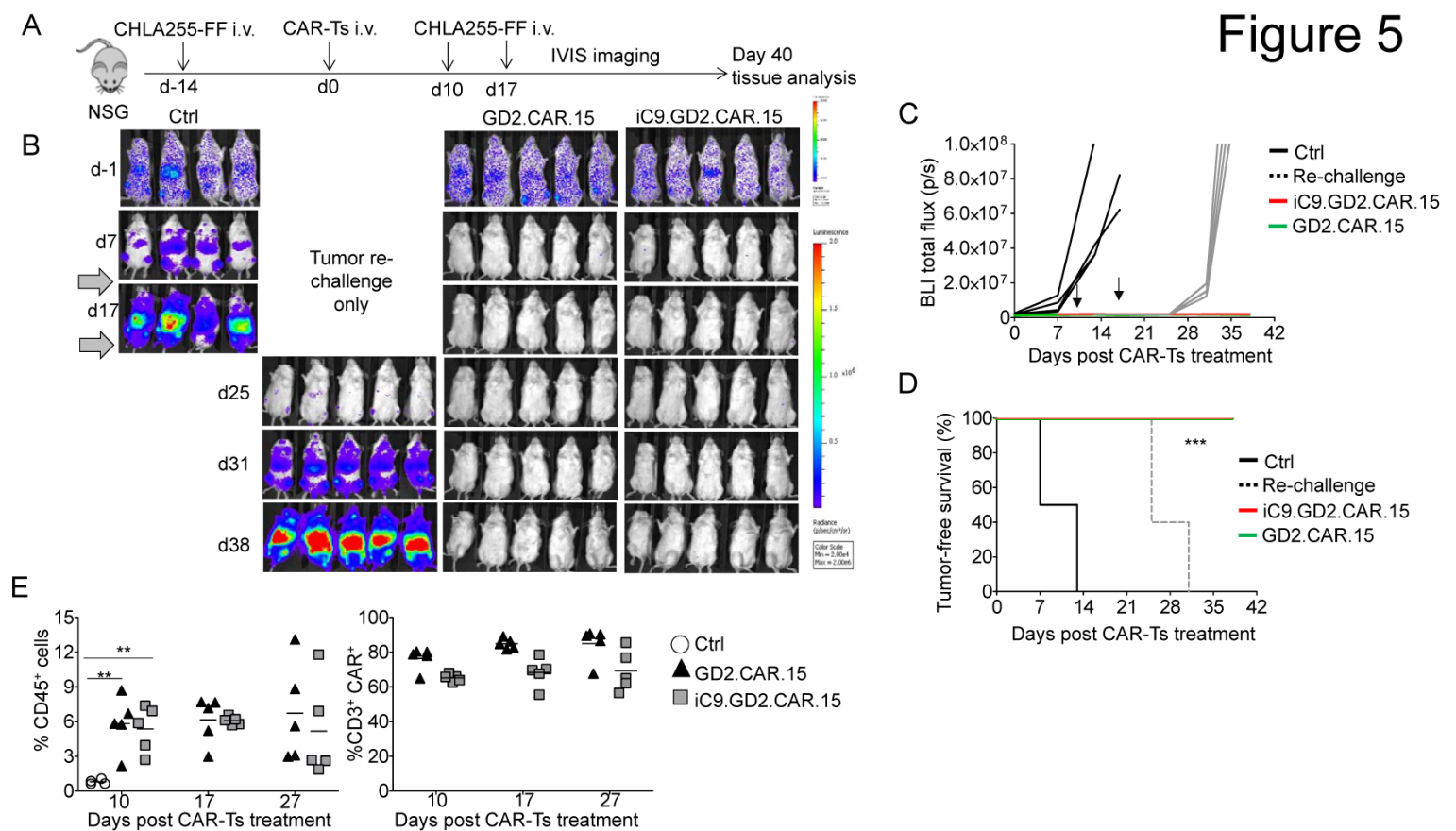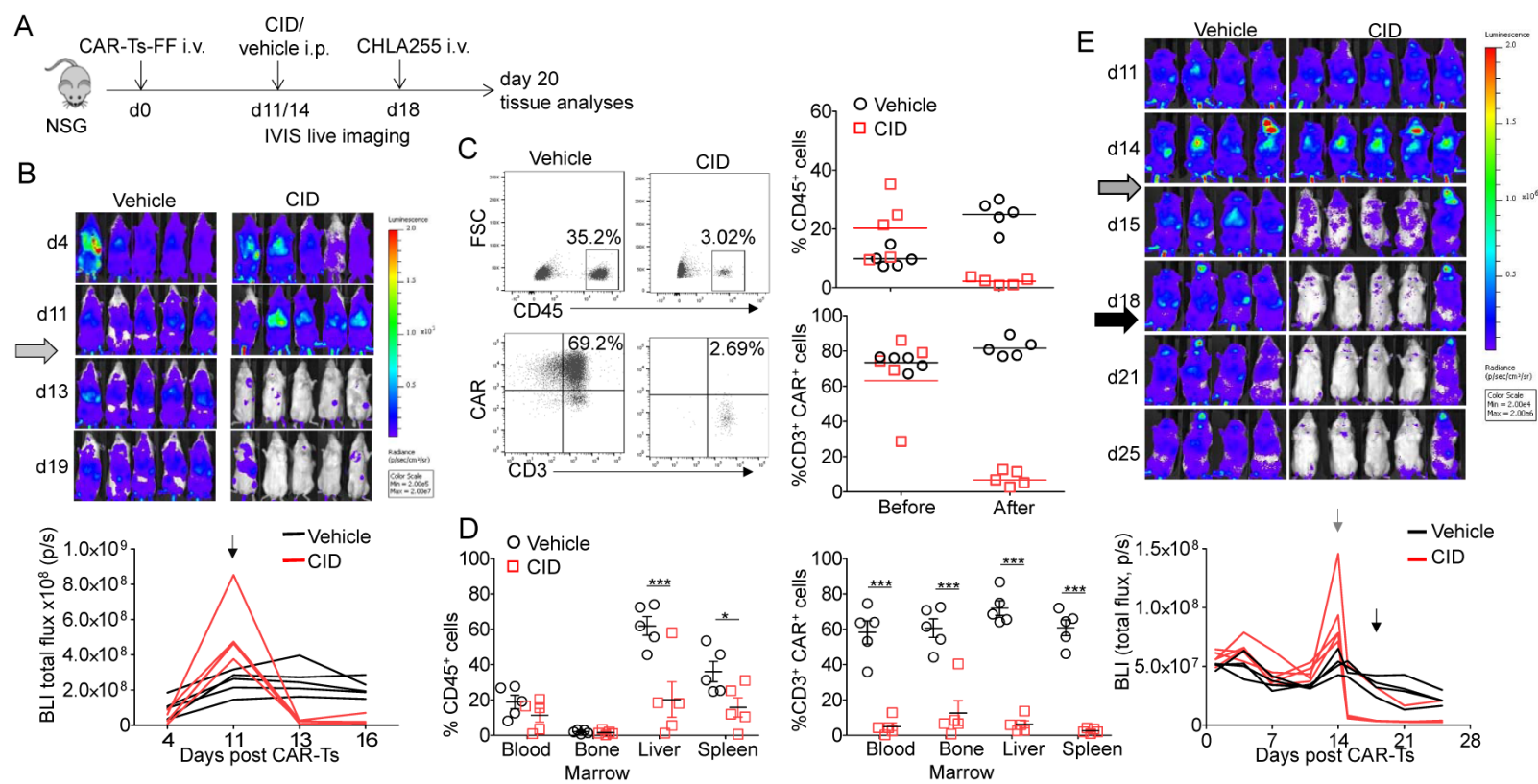
Clinical Cancer Research

Eradication of neuroblastoma by T cells redirected with an optimized GD2-specific chimeric antigen receptor and interleukin-15

Yuhui Chen, Chuang Sun, Elisa Landoni, et al.

Updated version	Access the most recent version of this article at: doi:10.1158/1078-0432.CCR-18-1811
Supplementary Material	Access the most recent supplemental material at: http://clincancerres.aacrjournals.org/content/suppl/2019/01/07/1078-0432.CCR-18-1811.DC1
Author Manuscript	Author manuscripts have been peer reviewed and accepted for publication but have not yet been edited.

E-mail alerts	Sign up to receive free email-alerts related to this article or journal.
Reprints and Subscriptions	To order reprints of this article or to subscribe to the journal, contact the AACR Publications Department at pubs@aacr.org.
Permissions	To request permission to re-use all or part of this article, use this link http://clincancerres.aacrjournals.org/content/early/2019/01/07/1078-0432.CCR-18-1811. Click on "Request Permissions" which will take you to the Copyright Clearance Center's (CCC) Rightslink site.